ROM SAF Report 15
Ref: SAF/ROM/METO/REP/RSR/015
Web: www.romsaf.org
Date: 11 April 2013

The EUMETSAT Network of Satellite Application Facilities

ROM SAF
Radio Occultation Meteorology

ROM SAF Report 15

Improvements to the ROPP refractivity and bending angle operators

Chris Burrows[1], Sean Healy[2] and Ian Culverwell[1]

[1] *Met Office, Exeter, UK*
[2] *ECMWF, Reading, UK*

Document Author Table

	Name	Function	Date	Comments
Prepared by:	C. Burrows	ROM SAF Project Team	11 April 2013	
Reviewed by:	J. Eyre	Head of SA, Met Office	29 Apr 2013	
Approved by:	K. B. Lauritsen	ROM SAF Project Manager	13 May 2013	

Document Change Record

Issue/Revision	Date	By	Description
Version 1.0	11 Apr 2013	CB	First draft
Version 1.1	29 Apr 2013	CB	Post-review corrections
Version 1.2	13 May 2013	CB	Editorial changes suggested by KBL

ROM SAF

The Radio Occultation Meteorology Satellite Application Facility (ROM SAF) is a decentralised processing centre under EUMETSAT which is responsible for operational processing of GRAS radio occultation data from the Metop satellites and RO data from other missions. The ROM SAF delivers bending angle, refractivity, temperature, pressure, and humidity profiles in near-real time and offline for NWP and climate users. The offline profiles are further processed into climate products consisting of gridded monthly zonal means of bending angle, refractivity, temperature, humidity, and geopotential heights together with error descriptions.

The ROM SAF also maintains the Radio Occultation Processing Package (ROPP) which contains software modules that will aid users wishing to process, quality-control and assimilate radio occultation data from any radio occultation mission into NWP and other models.

The ROM SAF Leading Entity is the Danish Meteorological Institute (DMI), with Cooperating Entities: i) European Centre for Medium-Range Weather Forecasts (ECMWF) in Reading, United Kingdom, ii) Institut D'Estudis Espacials de Catalunya (IEEC) in Barcelona, Spain, and iii) Met Office in Exeter, United Kingdom. To get access to our products or to read more about the project please go to: http://www.romsaf.org

Abstract

The current bending angle operator in the ROPP package (ROPP_FM module) is based on Healy & Thépaut[1]. This operator is also used operationally at the Met Office, ECMWF and other NWP centres. The Met Office bending angle innovation statistics have shown features which can be attributed to shortcomings in the assumption of exponentially varying refractivity between model levels when the spacing is large. However, when the level spacing is small, the exponential assumption is acceptable. Similar features can be observed in the refractivity statistics. This report aims to address these issues by proposing a more physical approximation to the refractivity as a function of height between model levels which can be used in the Abel integral to forward-model bending angles. Improvements in both the refractivity and bending angle biases are demonstrated, along with several approaches for implementing an improved bending angle calculation.

Contents

1 Introduction

Data assimilation is the process of producing a statistically optimal analysis which is used as an input to an NWP forecast system. The assimilation step blends information from observations and short range (e.g. 6-hour) forecast fields, i.e. the background. The assimilation of observations usually requires interpolation of the model state to the location of the observation and this requires assumptions to be made about how the the model state varies between the levels.

Radio occultation (RO) measurements have high vertical resolution[2], so similar considerations are required. In the case of refractivity assimilation, the observed refractivity values describe the atmosphere at particular points (with some degree of spatial correlation), so interpolation of refractivity to this point is necessary. Forward-modelled bending angles, however, depend on the entire model atmosphere above the tangent point[3]. For this reason, the variation of refractivity with height needs to be known between each pair of model levels from the tangent point to the top of the model in order for the Abel integral, which calculates bending angle from refractivity, to be evaluated.

The bending angle operator used at the Met Office is based on the approach by Healy & Thépaut[1]. This assumes exponentially varying refractivity, N, as a function of x between model levels i and $i+1$. The independent variable x is the product of the refractive index n and the distance from the local centre of curvature of the Earth r, i.e. nr:

$$N(x) \quad = \quad N_i \exp\left(-k_i \left(x - x_i\right)\right) \qquad \text{for} \quad x_i \leq x < x_{i+1} \tag{1.1}$$

where:

$$k_i = \frac{\ln\left(N_i / N_{i+1}\right)}{x_{i+1} - x_i} \tag{1.2}$$

This ensures continuity at the model levels: $N(x_i) = N_i$ and $N(x_{i+1}) = N_i \exp\left(-k_i \left(x_{i+1} - x_i\right)\right) = N_{i+1}$.

With some further approximations, this can be integrated in the Abel transform, resulting in a difference of error functions. To a first approximation the exponential assumption seems reasonable as the refractivity is given by:

$$N = c_1 \frac{P}{T} + c_2 \frac{P_w}{T^2} \tag{1.3}$$

where P is pressure, T is temperature, P_w is the partial pressure of water vapour and c_1 and c_2 are empirical constants (Smith & Weintraub)[4].

In a dry atmosphere, the first term in Eq. (1.3) effectively represents the mass field. Where the *temperature is constant*, the hydrostatic equation $\frac{dP}{dz} = -\rho g$ implies that P falls exponentially with height: $P(z) = P_i \exp\left(-\frac{gz}{RT}\right)$. Therefore, N also falls exponentially. If the spacing between model levels is sufficiently small, this assumption can produce reasonable refractivities between the levels, and hence bending angles. If the spacing is large, however, the innovation statistics show features which indicate failings of this assumption. This report aims to address refinements to the form of the refractivity with height used in the refractivity and bending angle forward models.

2 Refractivity

At the Met Office, refractivity used to be assimilated operationally, and the same exponential assumption (i.e. Eq. (1.1), but in terms of geopotential height) was applied to obtain the forward-modelled refractivity values at observed geopotential heights given forward-modelled refractivities on the two surrounding model levels. This is equivalent to performing a linear interpolation of $\ln(N)$:

$$N_{ob\_height} = \exp\left[F \ln(N_i) + (1-F) \ln(N_{i+1})\right] \tag{2.1}$$

where

$$F = \frac{Z_i - Z_{ob\_height}}{Z_{i+1} - Z_i} \tag{2.2}$$

With this assumption applied, the innovation statistics ($(O-B)/B$) are plotted in Figure 2.1 (all plots in this report have had Met Office quality control applied to reject potentially poor quality observations).

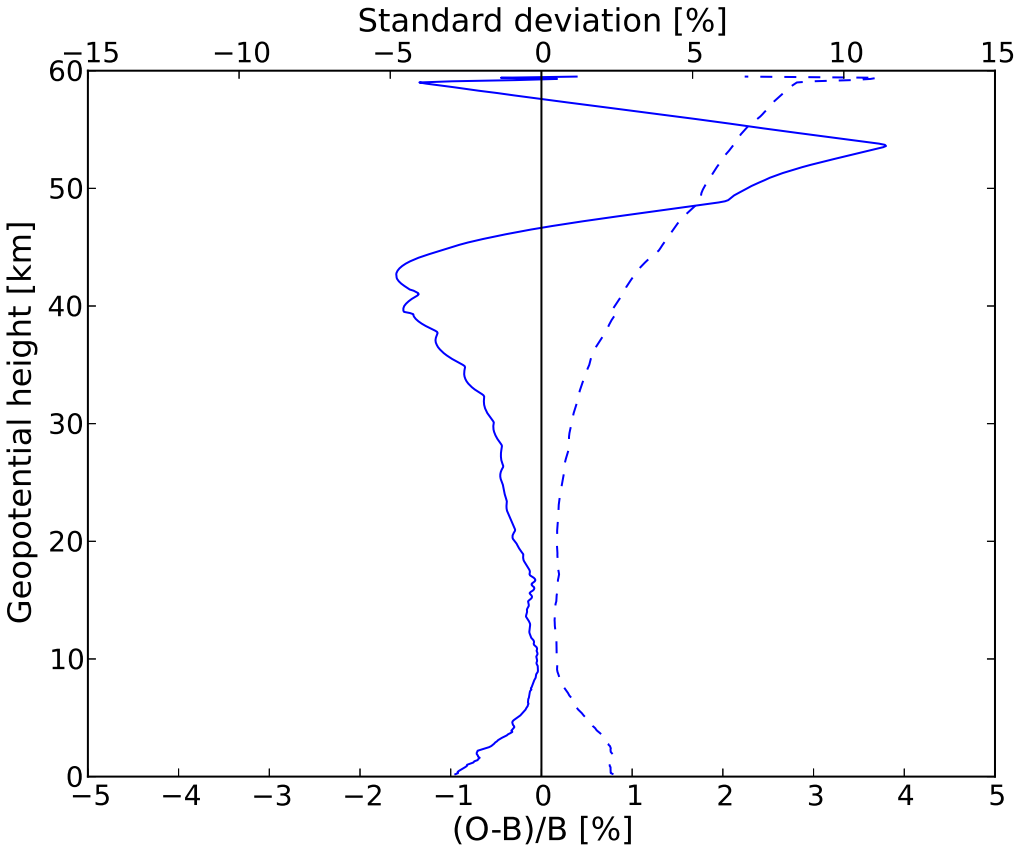

Figure 2.1: Refractivity innovations from 24 hours' worth of observation data from all available instruments starting from 15Z 15 August 2012. The refractivity between model levels is calculated using Eq. (1.3). [Solid is mean, dashed is standard deviation.]

To be clear on how this has been plotted, the values of $(O-B)/B$ are calculated for each observed profile, where $B = H(\mathbf{x})$, i.e. the forward-modelled refractivity values on observation levels ($\mathbf{x}$ is the

model background profile vector at the observation location and is on 70 levels). These are then linearly interpolated onto a fixed grid with spacing 100m. The statistics (mean and standard deviation) are calculated from these interpolated values.

The bias above $\sim 45\,\mathrm{km}$ should be ignored as it is due to a Met Office-specific model temperature bias. Similarly, the growing negative bias above $\sim 17\,\mathrm{km}$ relates, at least partly, to a bias arising from the handling of Met Office levels in the refractivity forward model. This broad bias is potentially more problematic, but is specific to the Met Office. The cause is understood and is being addressed. This broad bias is largely independent of the main topic of this report, and will be ignored to avoid complicating the discussion.

The general issue that will be addressed here is the small scale undulation that is present in the bias and is most noticeable between $25\,\mathrm{km}$ and $40\,\mathrm{km}$. The origin of these fluctuations becomes clear when the model levels are overlaid, Figure 2.2.

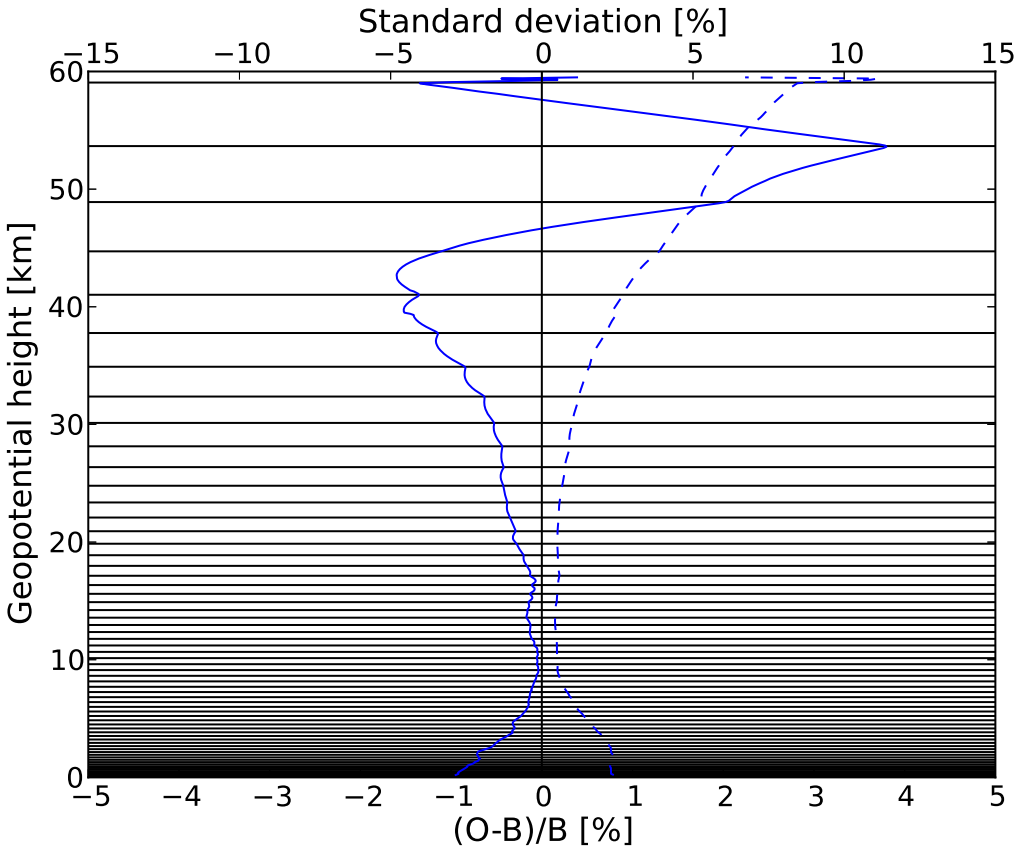

Figure 2.2: Refractivity innovations from 24 hours' worth of observation data from all available instruments (same data as Figure 2.1) with typical heights of the model levels overlaid. [Solid is mean, dashed is standard deviation.]

It can be seen that the magnitude of the oscillatory signal is smallest when the observations are close to the model levels and largest in between. Note that this is a real bias and not a feature of the plotting (the plotting routines have no knowledge of the heights of the model levels). In an assimilation system (3D-Var for simplicity), the cost function takes the form, in the usual notation:

$$J(\mathbf{x}) = \frac{1}{2}\left(\mathbf{x}_b - \mathbf{x}\right)^T \mathbf{B}^{-1}\left(\mathbf{x}_b - \mathbf{x}\right) + \frac{1}{2}\left(\mathbf{y} - H(\mathbf{x})\right)^T \mathbf{R}^{-1}\left(\mathbf{y} - H(\mathbf{x})\right) \tag{2.3}$$

where H is the non-linear forward-model operator. The second (observation) term includes the vector $\mathbf{y} - H(\mathbf{x})$ which is in observation space, and is identical to $O - B$ as used in the innovation statistics.

Therefore, the oscillations in the innovations will be present in this quantity, and hence they will introduce biases in the assimilation system.

The origin of these oscillations seems likely to be the exponential assumption between model levels overestimating the mid-layer refractivity.

3 Bending angle

The bending angle forward model is much more sensitive to subtle changes in the model background and the form of $N(x)$ which is integrated above the tangent point. This is because the bending angle is related to the vertical gradient of the refractivity. Therefore, it is no surprise that the bending angle statistics show the oscillatory bias even more strongly, Figure 3.1.

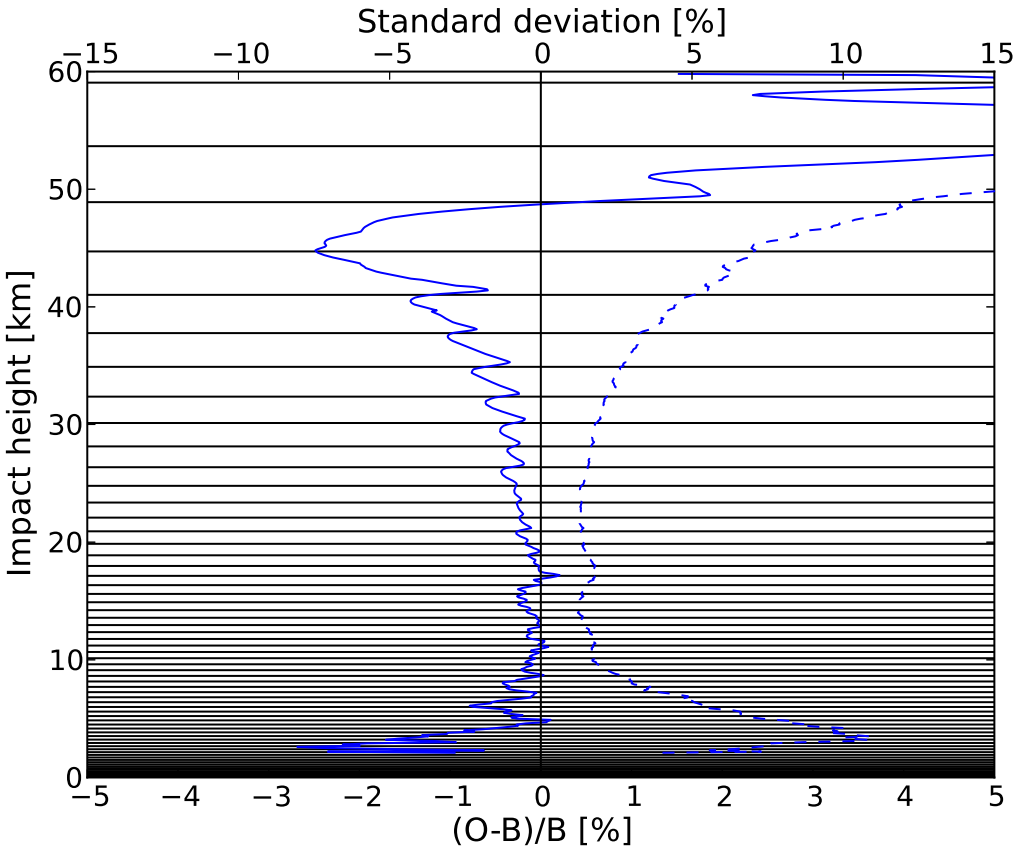

Figure 3.1: Bending angle innovations from 24 hours' worth of observations with typical heights of the model levels overlaid. The functional form of refractivity used is Eq. (1.1). Note that the model levels are plotted on geopotential heights and not impact heights. [Solid is mean, dashed is standard deviation.]

These statistics are calculated in a similar way to refractivity as above, but the values of $(O-B)/B$ for each profile are interpolated to a fixed grid of impact heights (impact parameter minus the local radius of curvature) rather than geopotential heights. These fixed heights are spaced by 100m. Using coarse binning (e.g. $1\,\mathrm{km}$) can hide these features, so we encourage other centres to follow this methodology to avoid overlooking these oscillations.

[As a brief aside, note that whilst for refractivity, the oscillations appear as small perturbations to the broad bias, for bending angles, the oscillations and broad bias have comparable magnitudes].

The bending angle as a function of impact parameter $\alpha(a)$ is given by the Abel integral[3, 5, 2]:

$$\alpha(a) = -2a \int_a^\infty \frac{\frac{d \ln n}{dx}}{\sqrt{x^2 - a^2}} dx$$

where $x = nr$ as before. By assuming exponential refractivity (and assuming $\sqrt{x^2 - a^2} \simeq \sqrt{2a}\sqrt{x - a}$), the bending angle contribution from a single layer is given by[1]:

$$\Delta\alpha_i = 10^{-6}\sqrt{2\pi a k_i} N_i \exp\left\{k_i \left(x_i - a\right)\right\} \left[\operatorname{erf}\left\{\sqrt{k_i \left(x_{i+1} - a\right)}\right\} - \operatorname{erf}\left\{\sqrt{k_i \left(x_i - a\right)}\right\}\right]$$

The implementation of the error function uses an accurate polynomial fit (Eqn 7.1.25 Abramowitz and Stegun[6]) to minimise the computational cost.

Because this is an integral from the tangent height upwards and is weighted most strongly close to the tangent point by the denominator, it makes sense that, if the assumption of exponential refractivity between model levels is sub-optimal, then the magnitude of the bias would be smallest close to the model levels, where $N(x)$ is most accurate, and largest in between, which can be seen in the plot. Interestingly, these oscillations do not appear so prominently in the equivalent statistics from ECMWF — it is thought that this is due to the higher vertical resolution in the stratosphere, compared to the Met Office, making the exponential assumption more accurate. This is discussed later in this report.

There are a number of possible approaches to improve on this assumption that will be considered here:

1. Use a more physical function of $N(x)$ as the best approximation, or "reference", between model levels and integrate this or an approximation to it.
2. Apply a simple polynomial correction term to the exponential to bring it closer to the "reference".
3. Use "pseudo-levels"; i.e. evaluate the "reference" on hypothetical intermediate levels and apply the existing exponential assumption to integrate between these model levels.

These methods all require a best guess for $N(x)$. This should preferably satisfy the following criteria:

- $N(x)$ should be continuous at model levels.
- It should have a physical basis.
- It should take information from as few model levels as possible.
- It should include atmospheric moisture.
- It should not be prohibitively costly.

3.1 Improved form of $N(z)$

A form of $N(z)$ used in Healy & Eyre[7] assumes exponentially varying specific humidity, linearly varying temperature and hydrostatic pressure. This form will be considered as the best guess, or "reference" refractivity between model levels in this report. The original paper used linear variation of the virtual temperature to obtain the hydrostatic pressure. Here, we use the temperature itself as even at the surface, the difference is rarely more than 1% and rapidly decreases with height, so in the upper-troposphere/lower-stratosphere, the differences will be very small. The specific humidity is, however, used in the moist term of the refractivity equation:

$$N(z) = c_1 \frac{P(z)}{T(z)} + c_2 \frac{P(z)Q(z)}{\left(\epsilon + (1 - \epsilon)\, Q(z)\right) T(z)^2} \tag{3.1}$$

where ϵ is the ratio of the molecular mass of water vapour and dry air and c_1 and c_2 are as in Eq. (1.3).

The specific humidity, temperature and pressure are defined as:

$$\begin{aligned} Q(z) &= Q_i \exp\left(\alpha_i (z - z_i)\right) \\ T(z) &= T_i + \beta_i \left(z - z_i\right) \\ P(z) &= P_i \left(1 + \frac{\beta_i}{T_i}(z - z_i)\right)^{-g/(R\beta_i)} \end{aligned} \tag{3.2}$$

Between model levels i and $i+1$, α_i is the vertical gradient of log(specific humidity) within the layer, β_i is the vertical gradient of temperature within the layer, g is the gravitational acceleration and R is the gas constant for dry air. Note that this form of $P(z)$ is different from what is assumed in a previous stage in the Met Office forward model for refractivity; in order to get all model variables on one set of the staggered levels, the Exner pressure values, $\Pi = (P/P_0)^{R/c_p}$, are interpolated linearly from their native levels. This discrepancy, along with the fact that the model is non-hydrostatic, results in the hydrostatic integral producing a discontinuity in N at the model levels, so a linear correction factor is applied to force the refractivity to be continuous:

$$N(z) = \left[c_1 \frac{P(z)}{T(z)} + c_2 \frac{P(z)Q(z)}{(\epsilon + (1-\epsilon)\,Q(z))\,T(z)^2}\right](1 + c\,(z - z_i)) \tag{3.3}$$

If the forward model handles the model variables consistently, this correction term should not be required. When Eq. (3.3) is used in the refractivity forward model, the vertical profile of the bias becomes significantly smoother, though a small oscillatory signal remains, Figure 3.2.

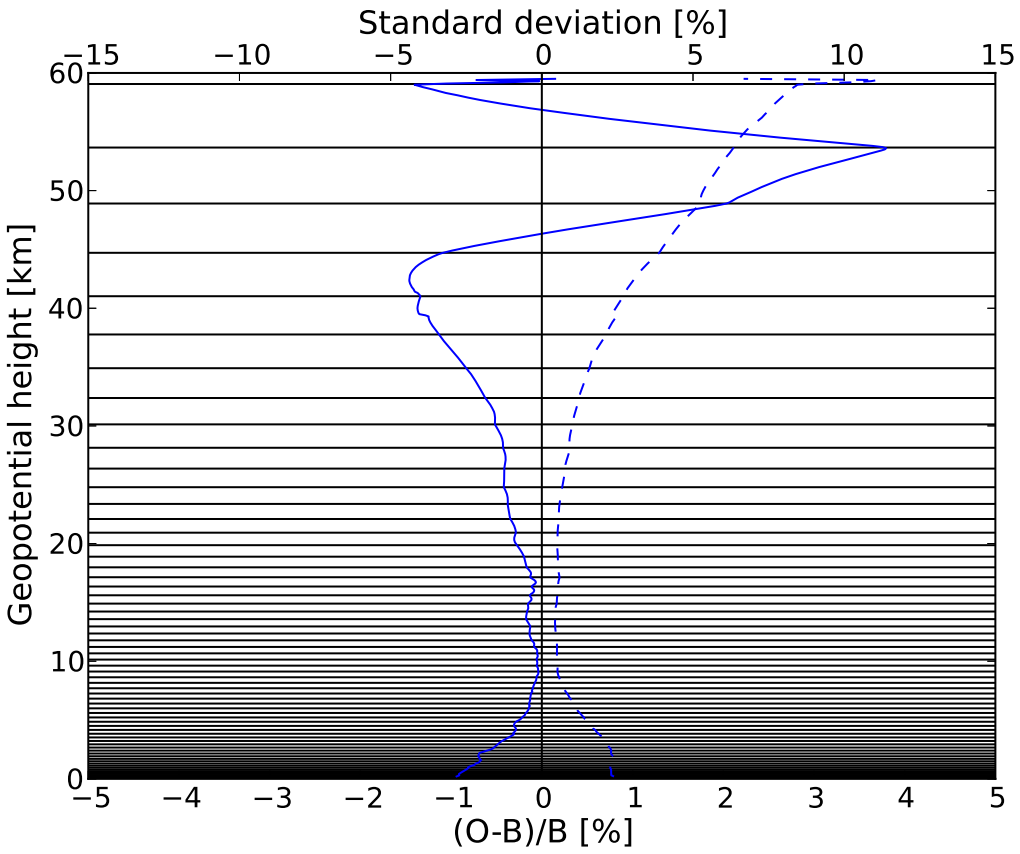

Figure 3.2: Refractivity innovations using the hydrostatic refractivity between model levels (Eq. (3.3)) with typical heights of the model levels overlaid. [Solid is mean, dashed is standard deviation.]

For bending angles, the independent variable is $x = nr = n(r_{curv} + z)$. Because the refractive index is close to unity even near the surface (where $n \simeq 1.0003$), the variation of the refractivity between model levels can reasonably be written in terms of $z - z_i$ or $x - x_i$ interchangeably. Also, the change to the vertical refractivity gradient arising from this change of variable has been investigated in computations for a small number of cases and the differences are small.

3.2 Options

Three possible approaches to implement an improved bending angle operator based on the hydrostatic form of the refractivity are presented here.

3.2.1 Expansion of $N(x)$

If we assume a dry atmosphere, the refractivity reduces to (in terms of x):

$$N(x) = N_i \left(1 + \frac{\beta_i (x - x_i)}{T_i}\right)^{-\frac{g}{\beta_i R} - 1} \quad \text{for} \quad x_i \leq x < x_{i+1} \tag{3.4}$$

The hydrostatic pressure will not be continuous between model levels, so a linear correction is applied to scale the function to preserve continuity of P and hence N:

$$N(x) = N_i \left(1 + \frac{\beta_i (x - x_i)}{T_i}\right)^{-\frac{g}{\beta_i R} - 1} (1 + c_i (x - x_i)) \tag{3.5}$$

where c_i in Eq. (3.5) is chosen to meet this condition for each layer.

This can be expanded in powers of $(x - x_i)$ to give a correction factor to the exponential:

$$N(x) = N_i \exp(-k_i (x - x_i)) \left[1 + A_i (x - x_i) + B_i (x - x_i)^2 + \ldots\right] \tag{3.6}$$

This functional form can also be obtained if instead it is assumed that k_i varies linearly within the layer. These two approaches, including the calculation of A and B are described in detail in the Appendix, and their resulting innovation statistics are almost identical. If the moist term is added, this form cannot be easily obtained. To use this dry form a cut-off height is needed (e.g. $15\,\mathrm{km}$), below which, an approach is used that does not require the assumption of a dry atmosphere, such as the existing exponential variation. At these heights, this assumption is reasonable as the model levels are more closely spaced. The innovation statistics using Eq. (3.6) and the coefficients from the second approach described in the Appendix up to the quadratic term in the series are shown in Figure 3.3:

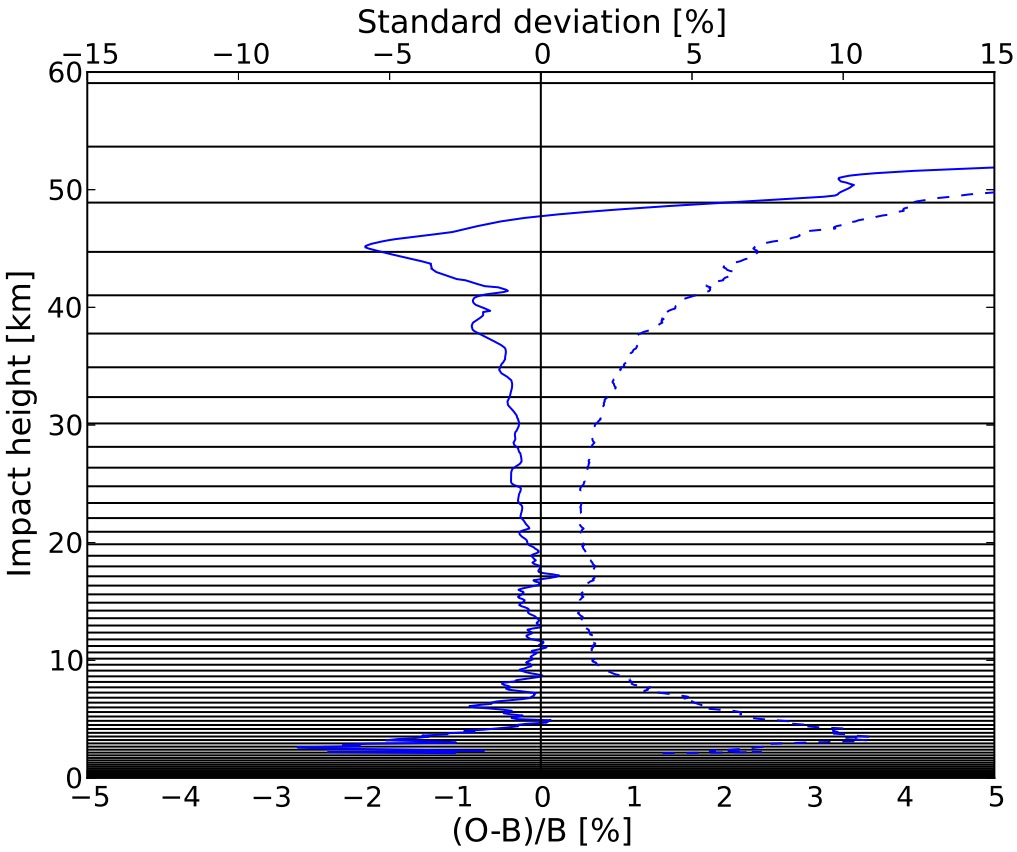

Figure 3.3: Bending angle innovation statistics using an integrable approximation to the dry hydrostatic refractivity, i.e. Eq. (3.6). [Solid is mean, dashed is standard deviation.]

The oscillations in the mean innovations are considerably reduced compared to Figure 3.1.

3.2.2 Polynomial correction

The exponential form of $N(z)$ can be modified by additional terms to better approximate the hydrostatic "reference" refractivity, including the moist term. For example:

$$N(z) = N_i \exp\left(-k_i \left(z - z_i\right)\right) + A_i \left(z - z_i\right) + B_i \left(z - z_i\right)^2 + \ldots \tag{3.7}$$

This could be used to give a very good approximation to the "reference" (if we know it), and can easily be integrated in the Abel transform, resulting in extra terms in addition to the error function. Figure 3.4 shows typical differences between the hydrostatic refractivity (Eq. (3.3)) and the exponentially varying refractivity between two model levels, as well as a quadratic approximation to this difference as described below. As a polynomial correction is a fit to the difference between the "reference" (i.e. the hydrostatic refractivity) and the exponential form, this difference must be evaluated at a number of points that is commensurate with the degree of the correction in order to fully determine the fit. For the quadratic example shown in Figure 3.5, the mid-layer difference between the corrected hydrostatic and exponential forms was used to provide the coefficients, along with ensuring continuity at the model levels.

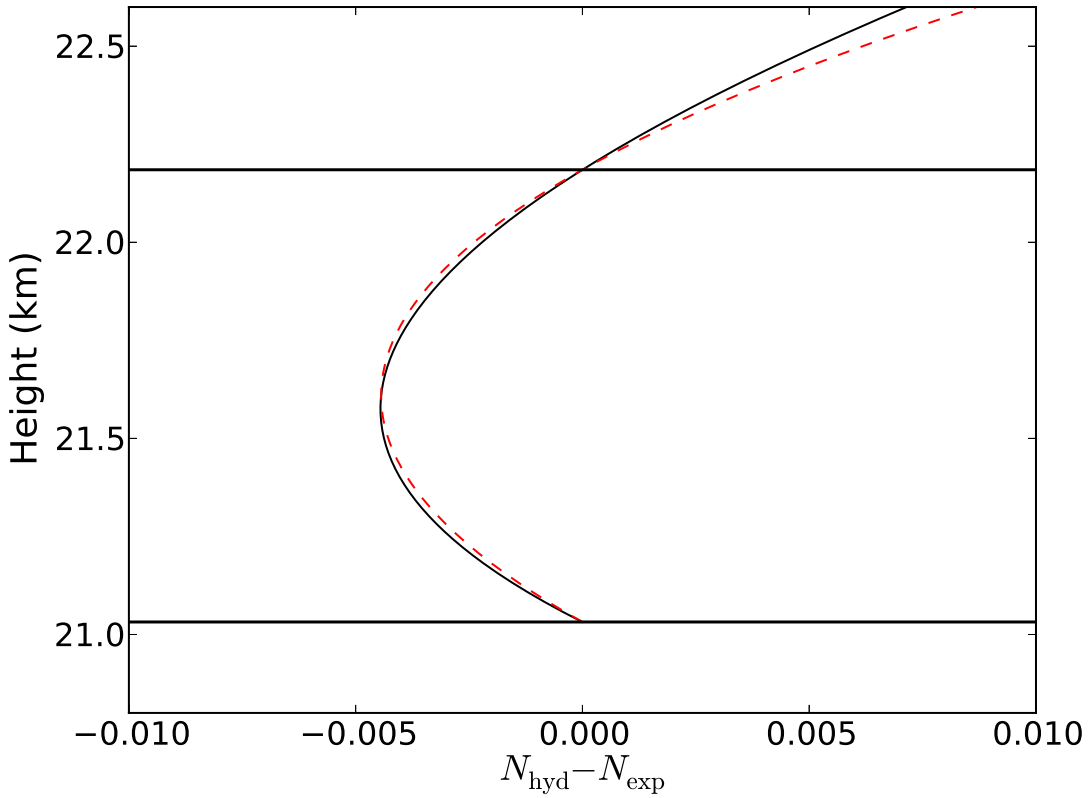

Figure 3.4: The difference of the corrected hydrostatic refractivity and the exponentially varying refractivity between a single pair of Met Office model levels (black). Also shown is a quadratic approximation to this difference (red dashed), as described in the text.

For continuity at z_{i+1}, the following relation must hold, since k_i is still given by Eq. (1.2):

$$A_i = -B_i \left(z_{i+1} - z_i\right) \tag{3.8}$$

The value of the quadratic at its turning point is set to be equal to the difference between the hydrostatic and exponential forms of the refractivity at the layer mid-point. This is reasonable to assume as from visual inspection the differences are approximately quadratic (Figure 3.4), and hence fairly symmetric about the midpoint. The turning point of the correction is found by setting the first derivative of the correction to zero:

$$0 = A_i + 2B_i \left(z - z_i\right) \tag{3.9}$$

If the turning point is close to the middle of the layer we can substitute 3.9 into the expression for the quadratic correction at the mid-point,

$$N_{\mathrm{hyd\_mid}} - N_{\mathrm{exp\_mid}} = -\frac{A_i^2}{2B_i} + \frac{A_i^2}{4B_i} \tag{3.10}$$

Substituting A_i from Eq. (3.8), we obtain a value for B_i:

$$B_i = -4 \left(N_{\mathrm{hyd\_mid}} - N_{\mathrm{exp\_mid}}\right) \frac{1}{z_{i+1} - z_i} \tag{3.11}$$

Inserting this form into the Abel integral results in an additional term in the expression for bending angle (having swapped $z - z_i$ for $x - x_i$ in an intermediate step):

$$\begin{aligned}\Delta\alpha &= 10^{-6}\sqrt{2\pi a k_i}N_i \exp\left[-k_i\left(x_i-a\right)\right]\left[\left\{\operatorname{erf}\sqrt{k_i\left(x-a\right)}\right\}\right. \\ &\quad \left. -2\times 10^{-6}\left\{\left(A_i-2B_i x_i\right)\ln\left(\sqrt{x^2-a^2}+x\right)+2C_i\sqrt{x^2-a^2}\right\}\right]_{x_i}^{x_{i+1}}\end{aligned} \tag{3.12}$$

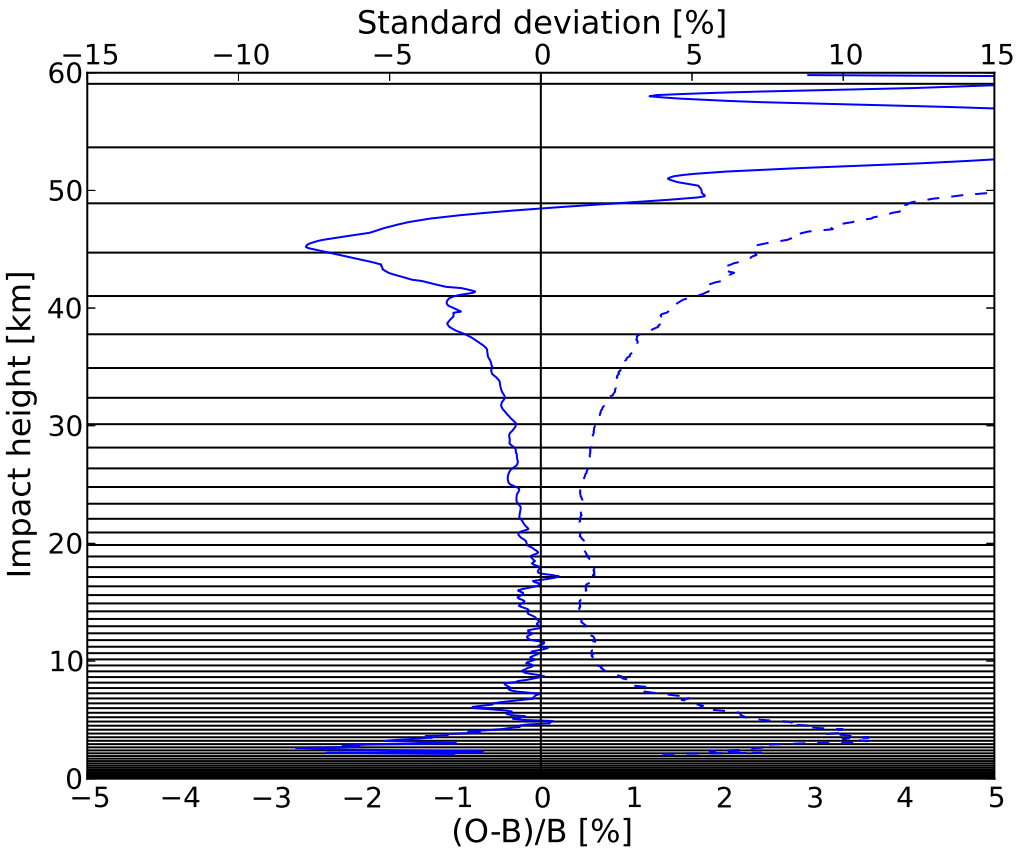

Figure 3.5: Bending angle innovation statistics, using an a quadratic adjustment to the exponential form of refractivity with height (Eq. (3.7)) to produce a better approximation to the hydrostatic form. [Solid is mean, dashed is standard deviation.]

This has been extended to include a cubic term to account for the small asymmetry in $N_{hyd} - N_{exp}$ at the mid-layer point. This does not show a significant improvement and leads to a more complicated form of the integral, so the results are not presented here.

3.2.3 Pseudo-levels

If the "true" refractivity, including the moist term, is evaluated at intermediate "pseudo-levels" which lie between the model levels (having first calculated Eqs. (3.2) on these pseudo-levels), then the exponential assumption can be accurately applied between these levels (if there are enough levels), so the current operator can simply be invoked multiple times within each model layer. For future changes, this is a flexible approach as the computation only needs to evaluate the refractivities on the pseudo-levels and the Abel integral remains unchanged, hence additional assumptions/simplifications can be avoided and a more sophisticated form could potentially be used. The number of pseudo-levels must be chosen to provide a balance between accuracy and computational cost. It has been found that using just one additional pseudo-level in the middle of each layer gives a good improvement for the

associated cost. Two or more equally spaced pseudo-levels only provide very small improvements to the innovation statistics for the single pseudo-level case, so results with just one pseudo-level will be presented here. For the layer in which the tangent point lies, the hydrostatic expression (Eq. (3.3)) is used to evaluate N at the tangent point, and at an additional pseudo-level halfway between the tangent point and the next highest model level. The resulting innovation statistics are shown in Figure 3.6.

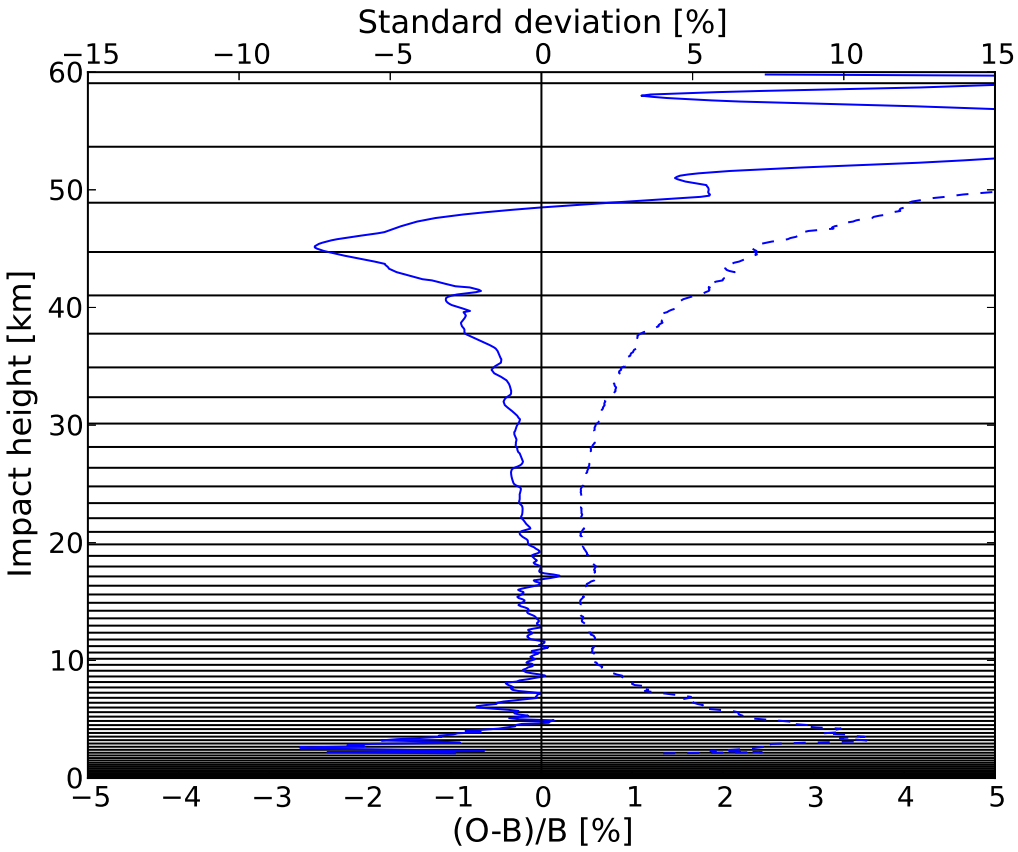

Figure 3.6: Bending angle innovation statistics, using hydrostatic refractivity (Eq. (3.3), including the moisture term) evaluated on one additional pseudo-level per model layer, and using an exponential function of refractivity with height to evaluate the Abel integral between the model/pseudo-levels. [Solid is mean, dashed is standard deviation.]

A further use of this method has been to examine the effect of "doubling" the number of model levels by introducing mid-layer pseudo-levels. This is similar to what is described above, but the treatment of the layer in which the tangent point lies is slightly different — the pseudo-level in this layer is at the layer's mid-point, rather than halfway between the tangent height and the next model level as was described above. The motivation for investigating this is to explain why the innovations from the L91 ECMWF system[8] do not show these oscillations as strongly as in the L70 Met Office[9] statistics. At a height of $35\,\mathrm{km}$, where the oscillations in the bias are prominent, the level spacing at ECMWF is $\sim 1.5\,\mathrm{km}$, and at the Met Office it is $\sim 2.9\,\mathrm{km}$, i.e. a factor of ~ 2 different. Figure 3.7 shows the innovations when pseudo-levels are used in this configuration.

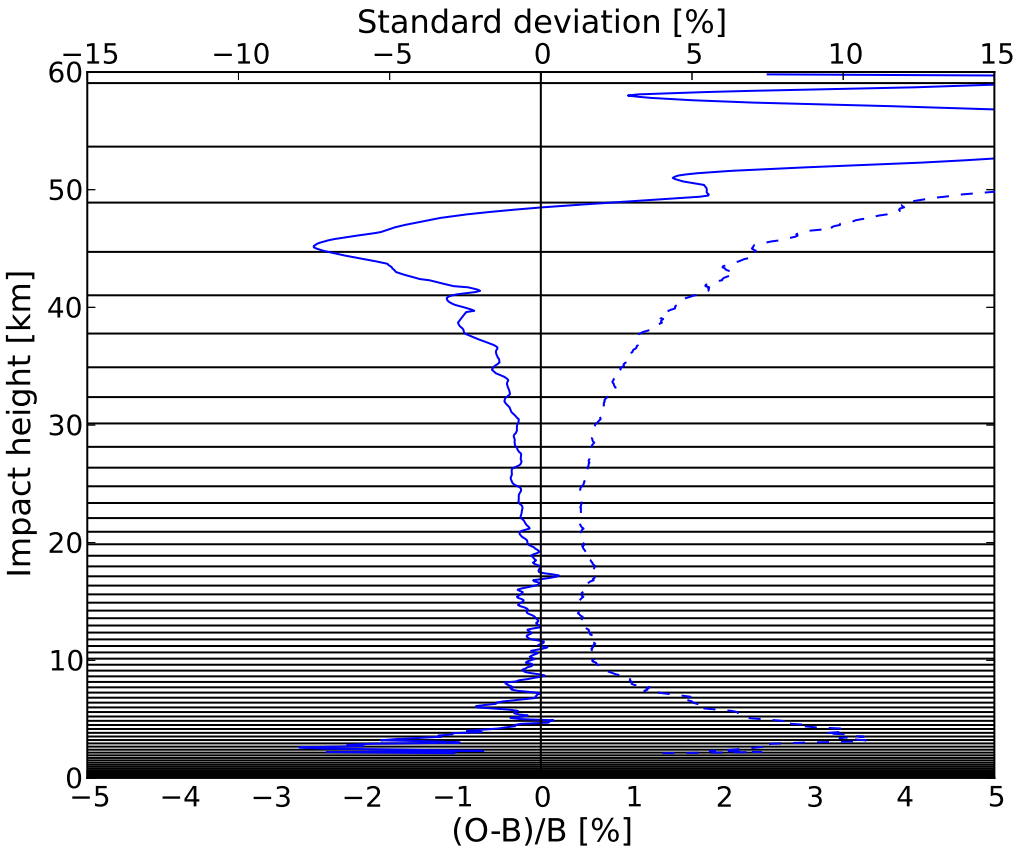

Figure 3.7: Bending angle innovation statistics, using hydrostatic refractivity (Eq. (3.3), including the moisture term) evaluated on a doubled-resolution vertical grid and using an exponential function of refractivity with height to evaluate the Abel integral between the model/pseudo-levels [Solid is mean, dashed is standard deviation.]

By comparing figures 3.7 and 3.1, it can be seen that by doubling the number of levels, the oscillations are reduced, and hence this provides an explanation as to why the ECMWF statistics do not display these features as strongly. In other words, the exponential assumption is more acceptable with the L91 resolution, but less so for L70. Another contributing factor is that the ECMWF height levels are more variable in this region than the Met Office levels and this could lead to smoothing out of the oscillatory signal, but this effect has not been investigated here.

4 Summary

It has been demonstrated that when model level spacing is large, the assumption of exponentially varying refractivity leads to systematic negative biases in refractivity and bending angle which are largest when the observation height lies between the model levels. The use of a more physical form of refractivity as a function of height has been investigated. This function assumes exponentially varying humidity, linearly varying temperature and hydrostatic pressure. Using this function, the magnitude of the oscillatory bias has been reduced considerably in both refractivity and bending angle statistics using Met Office background profiles. Three approaches to implement such an improvement have been suggested:

1. Integrate an approximation to the dry-hydrostatic refractivity analytically above a certain arbitrary level
2. Apply a polynomial correction to the exponential to make it a better approximation to the hydrostatic form
3. Evaluate the hydrostatic refractivity on mid-layer pseudo-levels and use the exponential function in the Abel integral between the model/pseudo-levels.

In the Appendix, two methods of approximating the dry hydrostatic form are given and the resulting bending angle statistics are consistent.

The results presented here should provide an important improvement to operational data assimilation systems. Usually, RO data is assimilated without a bias correction, and hence acts as an anchor to correct biased radiance observations. It is hoped that the reduction of this forward-model bias will improve analyses both directly and indirectly via bias correction schemes. Findings reported here could also be used in 1D-Var retrieval chains to improve the quality of the retrieved quantities.

Acknowledgements

This work was carried out as part of EUMETSAT's Radio Occultation Meteorology Satellite Application Facility (ROM SAF) which is a decentralised operational RO processing center under EUMETSAT.

5 Appendix — semi-analytical methods of evaluating the Abel integral for non-exponential $N(x)$

5.1 Form of $N(x)$ to be integrated

Between two model levels i and $i+1$, we currently assume:

$$N(x) = N_i\, e^{-k_i(x-x_i)} \tag{5.1}$$

where:

$$k_i = \frac{\ln\left(N_i/N_{i+1}\right)}{x_{i+1}-x_i} \tag{5.2}$$

It would be desirable to use the form of $N(x)$ given in Eq. (3.5), which guarantees continuity of N and obeys the hydrostatic equation, but this will not allow the Abel integral to be evaluated analytically, so a different approach is required. We achieve this by approximating the dry hydrostatic refractivity, $N(x)$, as the exponential form multiplied by an appropriate polynomial factor, $K(x)$:

$$N(x) = N_i\, e^{-k_i(x-x_i)} K(x) \tag{5.3}$$

To exactly reproduce the adjusted dry hydrostatic form, K must take the form:

$$K(x) = e^{k_i(x-x_i)} \left[\left(1 + \frac{\beta_i (x-x_i)}{T_i} \right)^{-\frac{g}{\beta_i R}-1} \left(1 + c_i\,(x-x_i)\right) \right] \tag{5.4}$$

Simplifying the notation with $X = x - x_i$ and $\gamma_i = \frac{g}{\beta_i R} + 1$:

$$K(x) = e^{k_i X} \left[\left(1 + \frac{\beta_i X}{T_i} \right)^{-\gamma_i} (1 + c_i X) \right] \tag{5.5}$$

A series expansion of this factor about $X = 0$ gives the following up to the quadratic term:

$$K(x) \simeq 1 + \left(-\frac{\beta_i \gamma_i}{T_i} + c_i + k \right) X + \frac{1}{2} \left(\frac{\beta_i^2 \gamma_i \left(\gamma_i + 1\right)}{T_i^2} - \frac{2\beta_i \gamma_i \left(c_i + k\right)}{T_i} + k\left(2c_i + k\right) \right) X^2 \tag{5.6}$$

Although this is an expansion of a continuous function, the truncation of the series will produce small discontinuities. Therefore, we again enforce continuity as follows:

$$K(x) \simeq 1 + \left(-\frac{\beta_i \gamma_i}{T_i} + c_i + k \right) X - \frac{1}{X_{i+1}} \left(-\frac{\beta_i \gamma_i}{T_i} + c_i + k \right) X^2 \tag{5.7}$$

where $X_{i+1} = x_{i+1} - x_i$ and c_i is:

$$c_i = \left[e^{-kX_{i+1}} \left(1 + \frac{\beta X_{i+1}}{T_i} \right)^{\gamma_i} \right] \frac{1}{X_{i+1}} \tag{5.8}$$

The form of the refractivity is, then:

$$N(x) = N_i\, e^{-k(x-x_i)} \left[1 + C_1\,(x-x_i) + C_2\,(x-x_i)^2 \right] \tag{5.9}$$

where

$$\begin{aligned} C_1 &= \left(-\frac{\beta_i\gamma_i}{T_i} + c_i + k\right) \\ C_2 &= \frac{1}{x_{i+1} - x_i}\left(-\frac{\beta_i\gamma_i}{T_i} + c_i + k\right) \end{aligned} \tag{5.10}$$

5.2 Evaluating the integral

With a few steps, this form of the refractivity with height can be inserted into the Abel integral. First, $\ln(n)$ is calculated:

$$\ln(n) \simeq n - 1 = 10^{-6}N = 10^{-6}N_i\, e^{-k(x-x_i)}\left[1 + C_1\,(x - x_i) + C_2\,(x - x_i)^2\right] \tag{5.11}$$

so, the numerator in the integrand of the Abel transform is:

$$\frac{d\ln(n)}{dx} = 10^{-6}N_i\, e^{k(x_i-a)}e^{-k(x-a)}\left[P_1 + P_2\,(x - a) + P_3\,(x - a)^2\right] \tag{5.12}$$

where the following coefficients have been found by expressing the polynomial factor in terms of $(x - a)$

$$\begin{aligned} P_1 &= C_1 - k - (2C_2 - C_1k)\,(x_i - a) - kC_2\,(x_i - a)^2 \\ P_2 &= 2C_2 - C_1k + 2kC_2\,(x_i - a) \\ P_3 &= -kC_2 \end{aligned} \tag{5.13}$$

By assuming that $\sqrt{x^2 - a^2} \simeq \sqrt{2a}\sqrt{x - a}$ (this is most accurate close to the tangent point), the contribution to the bending angle from a single model layer is given by:

$$\begin{aligned} \Delta\alpha = -10^{-6}\sqrt{2a}\, e^{k(x_i-a)} \Bigg[& \mathrm{erf}\left\{\sqrt{k\,(x - a)}\right\}\sqrt{\pi}\left(\frac{P_1}{k^{1/2}} + \frac{P_2}{2k^{3/2}} + \frac{3P_3}{4k^{5/2}}\right) + \\ & \sqrt{x - a}\, e^{-k(x-a)}\left(-\frac{P_2}{k} + \frac{P_3\,(-2k\,(x - a) - 3)}{2k^2}\right)\Bigg]_{x_i}^{x_{i+1}} \end{aligned} \tag{5.14}$$

5.3 Alternative approach

A slightly different approach can be used to obtain $d\ln n/dx$ in the form of Eq. (5.12). This method provides additional insight into the reasons for the large bias between model levels in the exponential approach. This formulation makes different assumptions, and it is encouraging that the two approaches produce near-identical results in the innovation statistics; the difference in mean innovations is generally less than $\sim 0.01\%$ and the difference in standard deviation is less than $\sim 0.002\%$ for the four cycles used in the bending angle statistics throughout this report.

Starting with the equation for dry refractivity without the adjustment for continuity (Eq. (3.4)), the refractivity gradient with height is:

$$\begin{aligned} \frac{dN}{dx} &= -\left(\frac{g}{RT(x)} + \frac{\beta_i}{T(x)}\right)N(x) \\ &= -k(x)N(x) \end{aligned} \tag{5.15}$$

where $N(x)$ is the refractivity at x, and $T(x) = T_i + \beta_i\,(x - x_i)$.

We currently assume a fixed k throughout the layer, computed as in Eq. (5.2). Call this k_m and assume that this value is valid at the *centre* of the model layer $x_m = (x_i + x_{i+1})/2$.

From Eq. (5.15), k is inversely proportional to temperature:

$$k = \frac{A}{T} \tag{5.16}$$

where A is just a constant. So,

$$\frac{dk}{dT} = -\frac{k}{T} \tag{5.17}$$

in the layer. The change in k can be written as

$$\begin{aligned} \delta k &= -\frac{k}{T}\delta T \\ &= -\frac{k}{T}\left[\beta_i\,\delta x\right] \end{aligned} \tag{5.18}$$

We can therefore approximate the variation of k within the layer as:

$$k(x) \simeq k_m - \frac{k_m\beta_i}{T_m}\left(x - x_m\right) \tag{5.19}$$

We then compute the refractivity expression for this $k(x)$:

$$\int \frac{dN}{N} = -\int \left(k_m - \frac{k_m\beta_i}{T_m}\left(x - x_m\right)\right) dx \tag{5.20}$$

so

$$\ln(N) = -\left(k_m\left(x - x_i\right) - \frac{k_m\beta_i}{2T_m}\left(x - x_m\right)^2 - d\right) \tag{5.21}$$

where d is a constant of integration. To get appropriate values at x_i and x_{i+1}

$$N(x) = N_i \exp\left(-k_m\left(x - x_i\right) + \frac{k_m\beta_i}{2T_m}\left(\left(x - x_m\right)^2 - d\right)\right) \tag{5.22}$$

where d is chosen to satisfy the boundary conditions.

$$d = \left(x_i - x_m\right)^2 = \left(x_{i+1} - x_m\right)^2 \tag{5.23}$$

so the refractivity is continuous at the model levels. If the second term in the exponential is small then we can approximate

$$N(x) = N_i \exp\left(-k_m\left(x - x_i\right)\right) \times \left(1 + \frac{k_m\beta_i}{2T_m}\left(\left(x - x_m\right)^2 - d\right)\right) \tag{5.24}$$

This makes the largest change to the pure exponential at the centre of the layer. The vertical gradient of $\ln(n)$ is

$$\frac{d\ln n}{dx} = N_i \exp\left(-k_i\left(x - x_i\right)\right)\left(-k_i - \frac{k_i^2\beta_i}{2T_m}\left(\left(x - x_m\right)^2 - d\right) + \frac{k_i\beta_i}{T_m}\left(x - x_m\right)\right) \tag{5.25}$$

which can be cast into the same form as Eq. (5.12), using the coefficients:

$$\begin{aligned} P_1 &= -\ k_i - \frac{k_i^2\beta_i}{2T_m}\left(\left(a - x_m\right)^2 - d\right) + \frac{k_i\beta_i}{T_m}\left(a - x_m\right) \\ P_2 &= -\frac{k_i^2\beta_i}{T_m}\left(a - x_m\right) + \frac{k_i\beta_i}{T_m} \\ P_3 &= -\frac{k_i^2\beta_i}{2T_m} \end{aligned} \tag{5.26}$$

Bibliography

[1] S. B. Healy and J.-N. Thepaut. Assimilation experiments with CHAMP GPS radio occultation measurements. *Quart. J. Roy. Meteorol. Soc.*, 132:605–623, 2006.

[2] E. R. Kursinski, G. A. Hajj, J. T. Schofield, R. P. Linfield, and K. R. Hardy. Observing earth's atmosphere with radio occultation measurements using the Global Positioning System. *J. Geophys. Res.*, 102:23.429–23.465, 1997.

[3] G. Fjeldbo, G. A. Kliore, and V. R. Eshleman. The neutral atmosphere of Venus as studied with the Mariner V radio occultation experiments. *Astron. J.*, 76:123–140, 1971.

[4] E. K. Smith and S. Weintraub. The constants in the equation for atmospheric refractivity index at radio frequencies. In *Proc. IRE*, volume 41, pages 1035–1037, 1953.

[5] W. G. Melbourne, E. S. Davis, C. B. Duncan, G. A. Hajj, K. R. Hardy, E. R. Kursinski, T. K. Meehan, and L. E. Young. The application of spaceborne GPS to atmospheric limb sounding and global change monitoring. Publication 94–18, Jet Propulsion Laboratory, Pasadena, Calif., 1994.

[6] M. Abramowitz and I. A. Stegun, editors. *Handbook of mathematical functions*. Dover, 1965.

[7] S. B. Healy and J. R. Eyre. Retrieving temperature, water vapor and surface pressure information from refractive–index profiles derived by radio occultation: A simulation study. *Quart. J. Roy. Meteorol. Soc.*, 126:1661–1683, 2000.

[8] ECMWF. IFS documentation - Cy31r1. Part III: Dynamics and numerical procedures. IFS documentation, ECMWF, 2007. http://ecmwf.int/research/ifsdocs/CY31r1/index.html.

[9] T. Davies, M. J. P. Cullen, A. J. Malcolm, M. H. Mawson, A. Staniforth, A. A. White, and N. Wood. A new dynamical core for the met offices global and regional modelling of the atmosphere. *Quart. J. Roy. Meteorol. Soc.*, 131:1759–1782, 2005.

ROM SAF (and GRAS SAF) Reports

SAF/GRAS/METO/REP/GSR/001	Mono-dimensional thinning for GPS Radio Occulation
SAF/GRAS/METO/REP/GSR/002	Geodesy calculations in ROPP
SAF/GRAS/METO/REP/GSR/003	ROPP minimiser - minROPP
SAF/GRAS/METO/REP/GSR/004	Error function calculation in ROPP
SAF/GRAS/METO/REP/GSR/005	Refractivity calculations in ROPP
SAF/GRAS/METO/REP/GSR/006	Levenberg-Marquardt minimisation in ROPP
SAF/GRAS/METO/REP/GSR/007	Abel integral calculations in ROPP
SAF/GRAS/METO/REP/GSR/008	ROPP thinner algorithm
SAF/GRAS/METO/REP/GSR/009	Refractivity coefficients used in the assimilation of GPS radio occultation measurements
SAF/GRAS/METO/REP/GSR/010	Latitudinal Binning and Area-Weighted Averaging of Irregularly Distributed Radio Occultation Data
SAF/GRAS/METO/REP/GSR/011	ROPP 1dVar validation
SAF/GRAS/METO/REP/GSR/012	Assimilation of Global Positioning System Radio Occultation Data in the ECMWF ERA-Interim Re-analysis
SAF/GRAS/METO/REP/GSR/013	ROPP PP validation
SAF/ROM/METO/REP/RSR/014	A review of the geodesy calculations in ROPP
SAF/ROM/METO/REP/RSR/015	Improvements to the ROPP refractivity and bending angle operators

ROM SAF Reports are accessible via the ROM SAF website: http://www.romsaf.org